Electronic Supplementary Material (ESI) for Nanoscale.

Supporting Information

Proton Intercalated Two-dimensional WO_3 Nano-flakes Window Enhanced Charge-carrier Mobility at Room Temperature

Serge Zhuiykov*, Eugene Kats, Benjamin Carey and Sivacarendran Balendhran

a

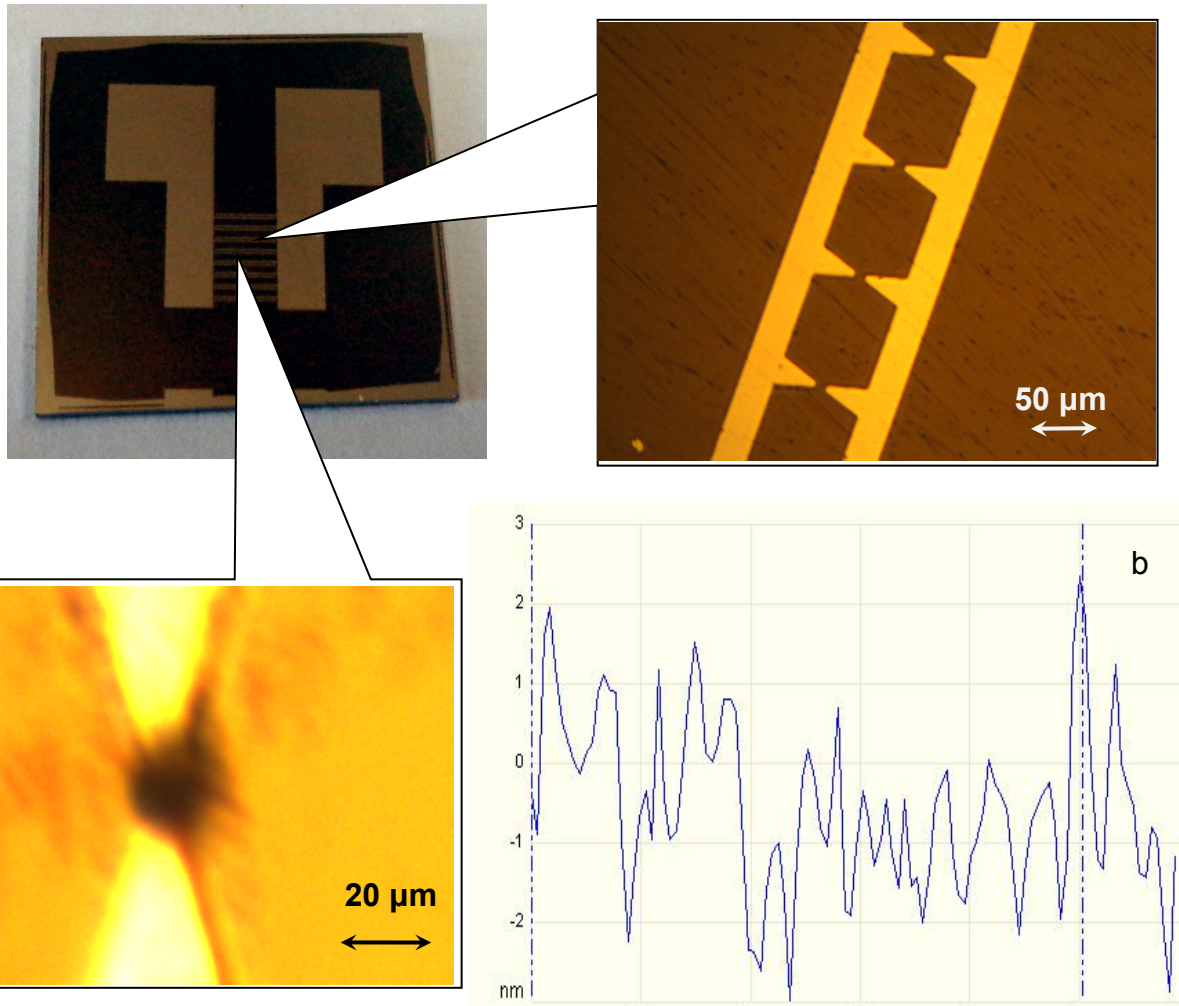

c

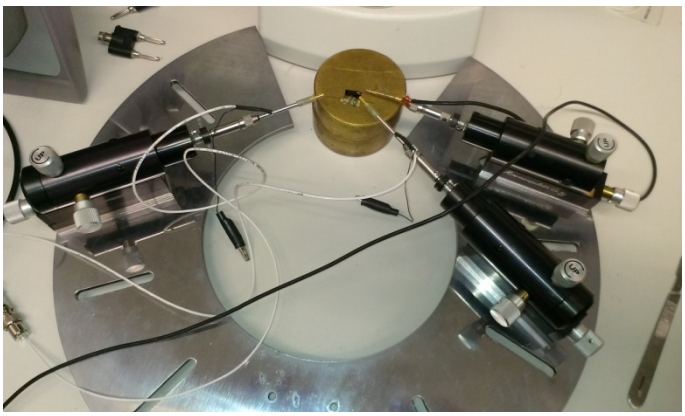

Figure S1. Optical images of SiO_2 substrate with applied Au/Cr electrodes and deposited Q2D WO_3 nano-flake (A), roughness measurement of SiO_2 substrate (B). Transistor function measurement setup (C).

Characterization of the Q2D WO_3 nano-flakes

The developed WO_3 nanostructures were characterised using scanning electron microscopy (SEM), X-ray diffraction (XRD), energy-dispersive X-ray spectroscopy (EDX), Fourier transform infra-red absorption spectroscopy (FTIR), Raman spectroscopy, atomic force microscopy (AFM), Raman spectroscopy and X-ray photoelectron spectroscopy techniques (XPS). The crystallinity of the developed WO_3 nano-flakes was characterized by RINT 2100VLR/PC, Rigaku X-ray diffractometer with CuKα radiation (α = 0.1542Å) at angle step of 1º min^{-1}. XRD intensities and records were collected using a scintillation detector, and each sample was scanned over the 2-theta range 10-80º. Spectral analyses were carried out using Bruker ZRD search match program – EVA™, and crystalline phases were analysed using the ICDD-JCPDS powder diffraction database. Both the surface morphology and structural configuration of Q2D WO_3 nano-flakes were evaluated by a Philips XL30 field emission SEM. Iridium coating was also applied to the sample to improve the quality of the imaging. All the measurements were completed at room temperature. Meanwhile, the local chemical homogeneity of the WO_3 nano-flakes were conducted by Type N energy dispersive X-ray spectrometer-EDX (Hitachi Science Systems Ltd., Japan) equipped with JOEL-JSM 5600 LV SEM. FTIR measurements were performed in air at room temperature by using Nicolet 6700 FTIR Spectrometer (Thermo Fisher Scientific, The Netherlands). Background gas for this examination was N_2. FTIR spectrometer had the following working parameters during the analysis: IR polarization – zero/no polarization; angle of incidence – 90° perpendicular to the sample; analysing material – KBr; type of detector – MCT detector. During each measurement the background spectrum was registered and consequently

subtracted from the sample spectrum captured to obtain the final spectra. These were studied by employing Omnic Spectroscopy Software Suite. All the spectra were acquired in the following range: 4000-400 cm^{-1}. Before experiments, WO_3 nanostructures were preheated to 200˚C for removal of adsorbed moisture and CO_2 and then cooled down to room temperature. For FTIR measurements Q2D WO_3 nano-flakes were also prepared on Au/Si substrate. Ultra-high clean N_2 was selected as a background gas. It was flowing through the cell containing WO_3 for 10 min with speed 100 ml/min. After that WO_3 nano-structures were exposed to the air for 10 min before any measurements commenced. At each experiment and evaluation, the background spectrum was recorded and subtracted from the sample spectrum obtained.

AFM measurements were performed to construct and identify the surface profile and simultaneously obtain typical topographical, tunnelling and current/voltage properties of the exfoliated Q2D WO_3 nano-flakes. This procedure was completed using Bruker MultiMode-8 Atomic Force System with installed Peak Force TUNA module (model: MM8-PFTUNA for MultiMode8 AFM system, Germany) and the data was analysed by employing NanoScope Analysis software. Raman Spectroscopy was used to determine and identify the vibration and rotation information regarding the chemical bonds. μSense-L-532-B Laboratory Raman Analyser (Warsash Scientific Pty Ltd) was employed for this purpose. During the testing CCD detector was cooled down to -60^{o}C. The spectra obtained were studied by RamanReader-M Software (Enwave Optronics Inc). Impedance measurements were conducted using a frequency response analyser (AUTOLAB-PGSTAT30, Echo-Chemie, The Netherlands) at a room temperature. XPS measurements (VG MicroLab VG-310G) are performed using Al non-monochromated X-ray (20 kV, 15 mA) with the hemispherical energy analyser set at a pass energy of 20 eV for the peak scans. The absorbance spectra of Q2D WO_3 nano-flakes are examined employing UV-Vis-NIR microspectrophotometer (CRAIC 20/30 PV). *I-V* characteristics of Q2D WO_3 nano-flakes were obtained at room

temperature using M&M Micromanipulator, Model 550, Agilent Technologies digital multimeter, Model 34411A, ETabor Electronics precision source/measurement unit, Model B2912A and 100 MHz Function/Arbitrary generator.

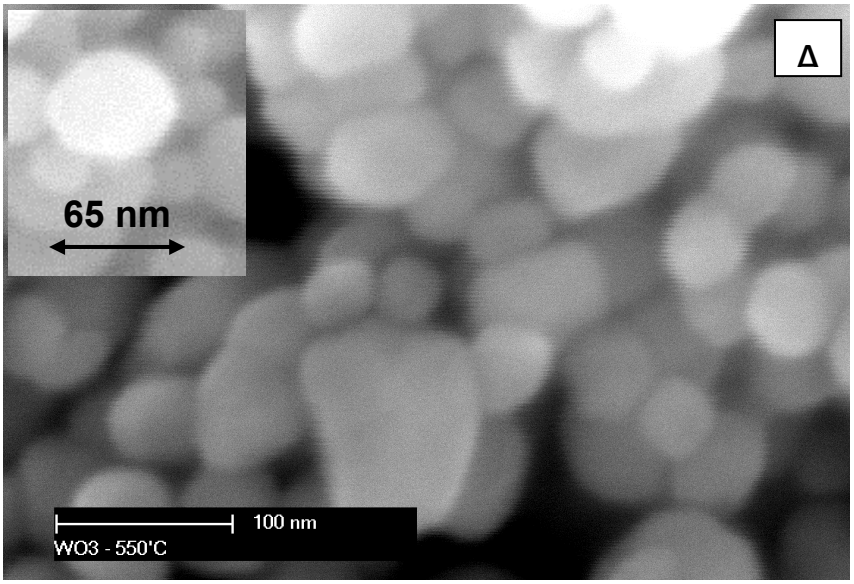

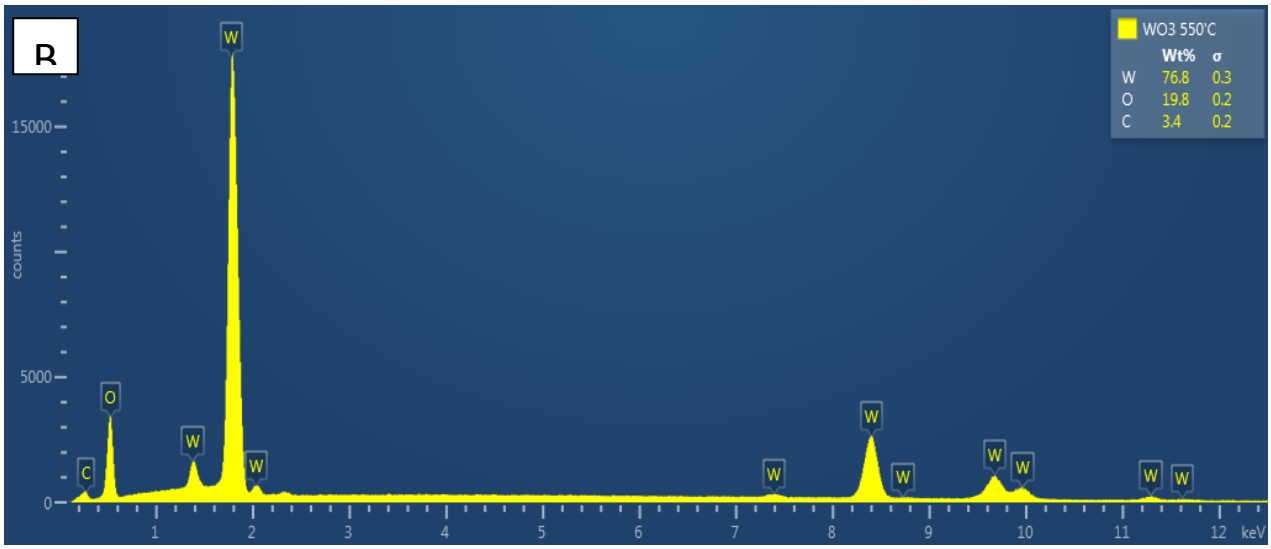

Figure S2. SEM image of the surface morphology of WO_3 nano-flakes sintered at 550ºC on SiO_2 substrate (A). Insert – typical WO_3 nano-flake. EDX analysis of WO_3 annealed at 550ºC (B).

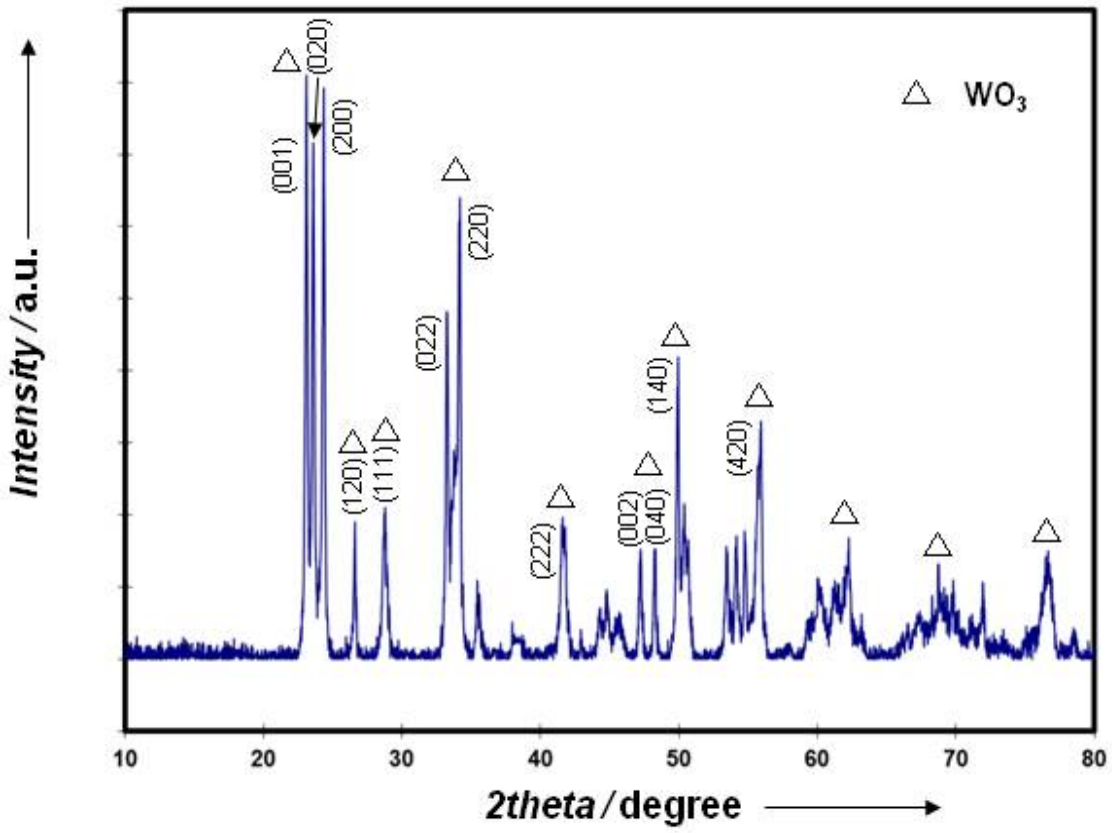

Figure S3. XRD patters of the WO_3 thin films sintered on Au-covered SiO_2 substrate at temperature of 550ºC.

AFM measurements

Morphological and electrical AFM measurements (Peak Force TUNA™) are carried out using appropriate modules equipped with current amplifier electronics yielding similar sensitivity (below 100 fA). All images are recorded under ambient conditions. In Conductive AFM (TUNA mode), Pt/Ir coated probes with a spring constant around 0.5 N/m are used for very soft contact between the tip and the sample. For electrical measurements, the samples are connected to the sample holder with silver paint.

The bearing curve is the integral of the surface height histogram and plots the percentage of the surface above a reference plane as a function of the depth of that below the highest point of the image. Bearing analysis has also confirmed that exfoliation removes large nano-agglomerations from the surface of the WO_3 nano-structures and at the same time reduces the

thickness of the WO_3 nano-flakes. Summarised data of bearing analysis for two exfoliated Q2D WO_3 nano-flakes with thickness of 2.5 and 4.0 nm are presented in Table S1.

Table S1. Results of bearing analysis of exfoliated WO_3 nano-flakes with measured thickness of 4.0 and 2.5 nm.

N/N	Results	WO_3 nano-flake with thickness 4.0 nm	WO_3 nano-flake with thickness 2.5 nm
1	Bearing area	1,464.40 nm^2	291,298 nm^2
2	Bearing area percent	87.0483 %	83.1965 %
3	Bearing depth	4.13351 nm	1.46694 nm
4	Bearing volume	9,514.03 nm^3	596,813 nm^3
5	Box area	1,682.28 nm^2	350.133 nm^2
6	Centre line average	1.74382 nm	0.974142 nm
7	Histogram area	10.6785 nm^2	0.718748 nm^2

Impedance measurements

The impedance measurements were performed at the room temperature and at zero potential versus RHE. Q2D WO_3 sintered at 550ºC and intercalated sub-stoichiometric Q2D WO_{3-x} nano-flakes were used in these measurements. AC impedance measurements were done from 10^6 to 0.1 Hz. The series resistance are 1.5 Ω for Q2D WO_3 and 1.8 Ω for Q2D WO_{3-x}. It was fund that there is no significant difference between the Q2D WO_3 impedance and the intercalated non-stoichiometric Q2D WO_{3-x} impedance. The impedance primarily comes from wiring (e.g. cables, alligator clips) and the electrolyte, where the impedance of Q2D WO_3 or Q2D WO_{3-x} nano-flakes is negligible.

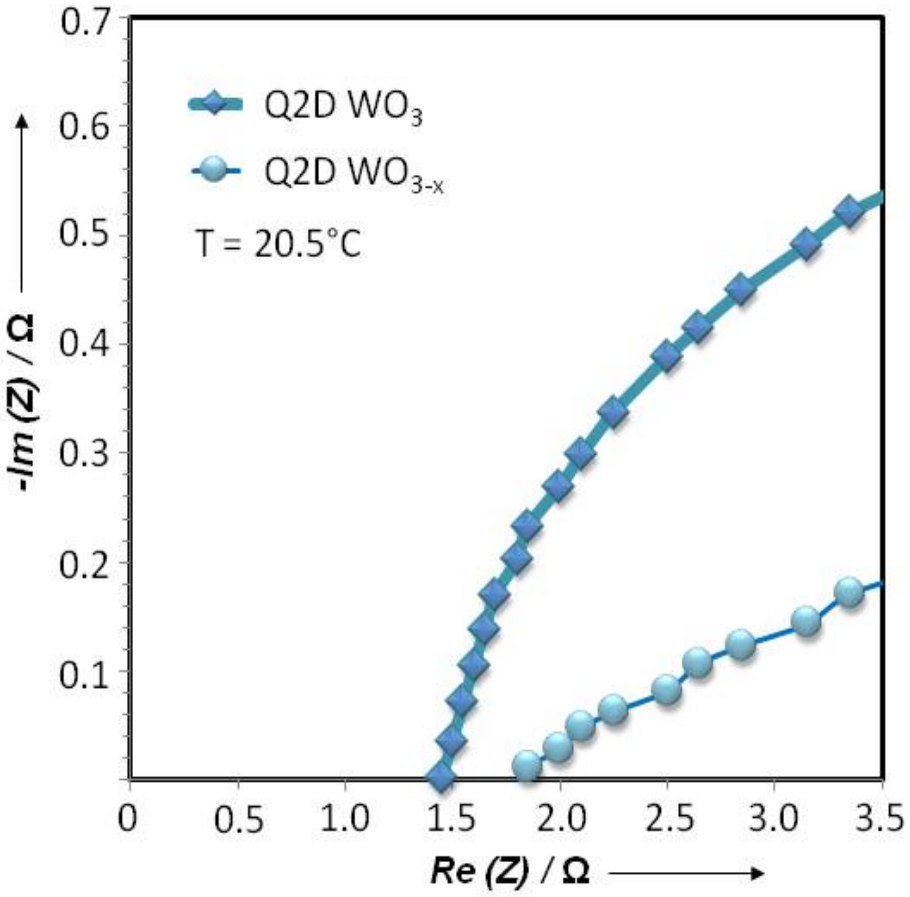

Figure S4. Nyquist plots of Q2D WO_3 and intercalated sub-stoichiometric Q2D WO_{3-x} nano-flakes.

Calculation of the charge mobility

The charge mobility in a thin nano-flake is calculated using $\mu = \frac{e}{m^2}\langle\tau\rangle,$ in which e is the point charge, is the transport relaxation rate of momentum in the plane, and m^* is the electron effective mass. Considering Born approximation, the transport relaxation time is calculated using: [1]

$$\frac{1}{\tau(E_k)} = \frac{2\pi}{\hbar}\sum_{k_z}\sum_{\mu}\int_{-\infty}^{+\infty} N_i^{(\mu)}(z)\left|V_{k-k_z}^{(\mu)}(z)\right|^2\left(1-cos\theta_{kk_z}\right)\delta\left(E(k)-E(k_z)\right), \quad (1)$$

where $N_i^{(\mu)}(z)$ is the concentration of the μ[th] kind of Coloumb charge centre and θ_{kk_z} is the angle between k and k_z vectors. $V_{k-k_z}^{(\mu)}(z)$ is a potential function showing the intensity of the

scattering effects on free mobile charges, and the reduction of $V_{k-k_z}^{(\mu)}(z)$ is important in obtaining large carrier mobilities. The term $V_{k-k_z}^{(\mu)}(z)$ is a function of many parameters of the material and uts surrounding environment such as permittivity, temperature, Q2D material thickness, embedded charges, and electronic structure of material. Its presence provides many degrees of freedom for manipulating of the Q2D material. For example, in such metal oxide as WO_3, which possesses high relative dielectric constant, the overall effect of Coloumb charges on $V_{k-k_z}^{(\mu)}(z)$ is reduced and according to Equation 1 the scattering effect will be dominated by the optical and acoustic phonons. This is due to the fact that in a Q2D semiconductor the permittivity appears in the denominator of the potential function[2]. For instance, for Q2D semiconductor with *k* of 5 and thickness of 11 nm, the calculated mobility is approximately ~170 $cm^2V^{-1}s^{-1}$ at the room temperature[2], whilst for semiconductor material of the same thickness and a high-*k* of 500, this number increases to ~3200 $cm^2V^{-1}s^{-1}$, which is limited by acoustic scattering rather than Coloumb scattering.[3]

Carrier mobility of the FET based on Q2D WO_3 nano-flakes was calculated using measured *I-V* characteristics using the following equation: [4]

$$\mu = \frac{\Delta I_{DS}}{\Delta V_{DS}} \times \frac{l}{C \times w \times V_{DS}} \quad , \qquad (2)$$

where $\frac{\Delta I_{DS}}{\Delta V_{DS}}$ is the transconductance defined by the drain-source current (I_{DS}) and gate-source voltage (V_{DS}), l = 12.0 μm is the channel length, w = 400 nm is the channel width, C = 1.15 × 10^{-8} F cm^{-2} is capacitance per unit area of the gate dielectric material, and V_{DS} = 0.8 V is the drain-source voltage. The surface charge density for exfoliated Q2D WO_3 nano-flake with thickness of 10 nm was calculated to be 275 $cm^2V^{-1}s^{-1}$, whereas the surface charge density for exfoliated and H^+ intercalated Q2D WO_3 nano-flake with same thickness was determined to

be 319 $cm^2V^{-1}s^{-1}$. The observed increase in the mobility can be related to the sub-stoichiometric layer introduced by the oxygen vacancies caused by the H^+ intercalation.

Throughout the transistor function measurements for Q2D WO_3, it was experimentally established that the built-up of charge on the measuring probe was accumulated. Therefore, instantaneous discharging had to be performed to bring the starting current back to zero prior to the commencement of each test. The experimental I_{DS}-V_{GS} data and graphs were relatively unstable at V_{DS} from 20 to 500 mV due the high background noise level. Therefore, only at V_{DS} = 0.8V stable and reliable measurements were obtained.

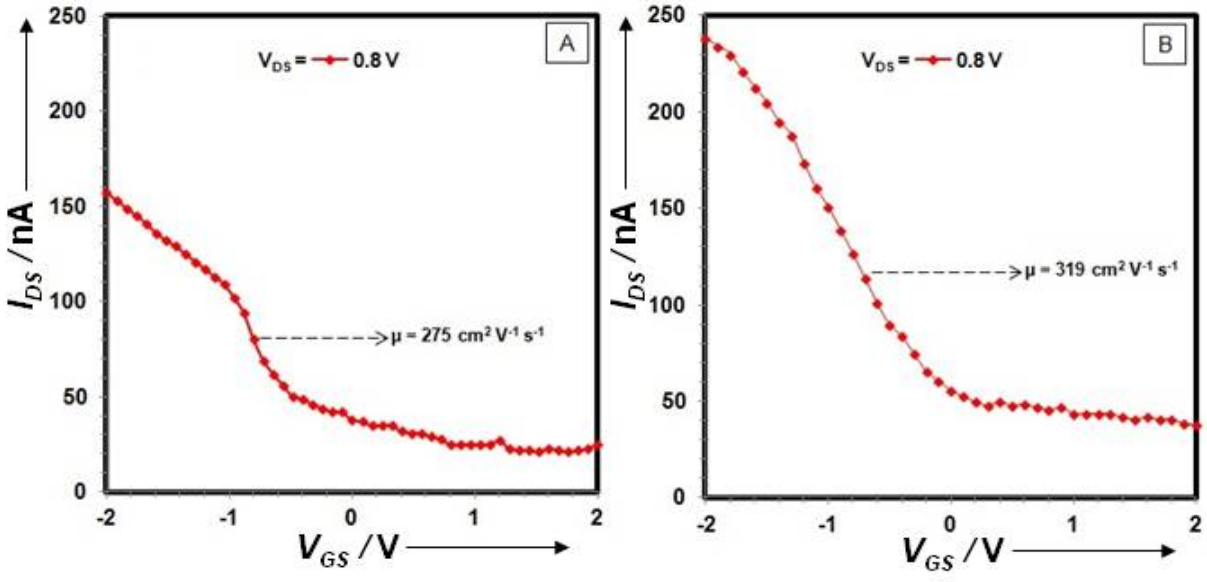

Figure S5. Experimental I_{DS} *vs* V_{DS} characteristics for the FET device based on exfoliated Q2D WO_3 at V_{DS} = 0.8V (a). Experimental I_{DS} *vs* V_{DS} characteristics for the FET device based on exfoliated and H^+ intercalated Q2D WO_3 sub-stoichiometric WO_{3-x} (b).

FTIR measurements

In-situ FTIR spectroscopy of exfoliated Q2D WO_3 and H^+ intercalated WO_{3-x} was utilised to determine surface chemistry and surface reactions of the developed nano-flakes and results are presented in Fig. S6. They illustrate the bonding characteristics of the functional groups in exfoliated Q2D WO_3 and intercalated WO_{3-x} nano-flakes. The higher surface area enables the

detection of bands owing to surface OH and adsorbed water in the 3700-3100 cm^{-1} region (not shown in presented Fig. S6). Specifically, for both Q2D WO_3 and WO_{3-x} the sharp peaks at 1620 cm^{-1} are various O-H stretching modes due to H_2O bending mode. Generally about 40% of the total adsorbed water remains strongly bound to the surface up to 150ºC. Weak C-H stretching modes at 2991 cm^{-1} were also observed.

Considering that WO_3 contains cations in the highest degree of oxidation (+6), CO molecules do not adsorb on its surface because of full coordination. The frequency values obtained in spectra of CO adsorbed on Q2D WO_3 nano-flakes shifted to the lower values compared to the assignments represented for micro-structured WO_3. [5] This is connected with the fact that in the analysed exfoliated Q2D WO_3 nano-flakes the degree of oxidation on some parts of the WO_3 surface has been changed and few WO_{3-x} sites appeared on the surface of nano-flakes causing CO adsorption. Due to the development of oxygen vacancies in intercalated WO_{3-x} the intensity of C=O peak is higher. It should be also noted that some residual hydrated WO_3 is most likely present in the sample because hydrated WO_3 is formed in the sol-gel process and then converted to β-WO_3 during sintering.[6,7] In the obtained spectra the peaks in the fingerprint region, namely at 1048 and 1161 cm^{-1}, are assigned to stretching mode of W-O, whereas the stretch at 984 cm^{-1} is due to W=O vibrations. The W-O stretching modes are less intense, and changes in the low-frequency modes may indicate some modifications in the tungsten-oxide framework. This is possibly owing to the fact that the surface of exfoliated Q2D WO_3 itself contains various defects. The intensity of W-O stretching mode even lower for intercalated WO_{3-x}. In general, the majority of experimental phenomena discussed above were associated to adsorption on expected sites of oxide nano-flake surface (co-ordinatively unsaturated cations, hydroxyls and their pair). However, the appearance of the most active surface centres suggests a connection with defects in nano-flakes.[5,8] The other factors influencing properties of the *"real"* oxide surfaces are (i) the presence of different lattice

defects in the surface layer of nano-flake, and (ii) their chemical composition, which differ after intercalation process. There was also one stretch observed at 1265 cm^{-1} (Si), which directly relates to the substrate platform. The WO_3 FTIR spectra also indicated that there were no impurities in Q2D exfoliated and H^+ intercalated samples. Based on the above-mentioned Raman spectra and curve fitting results, it can be concluded that the Raman intensity change of the measured peaks were directly affected by hydration level of the film after H_2 gas exposure. In addition, Opara-Krasovec *et al.* have independently concluded by *in-situ* IR spectroscopic studies of WO_3 film synthesized using sol-gel method upon H_2 gas exposure that the existence of surface water molecules and the electronic transitions involving W^{6+}/W^{5+} redox changes.[9]

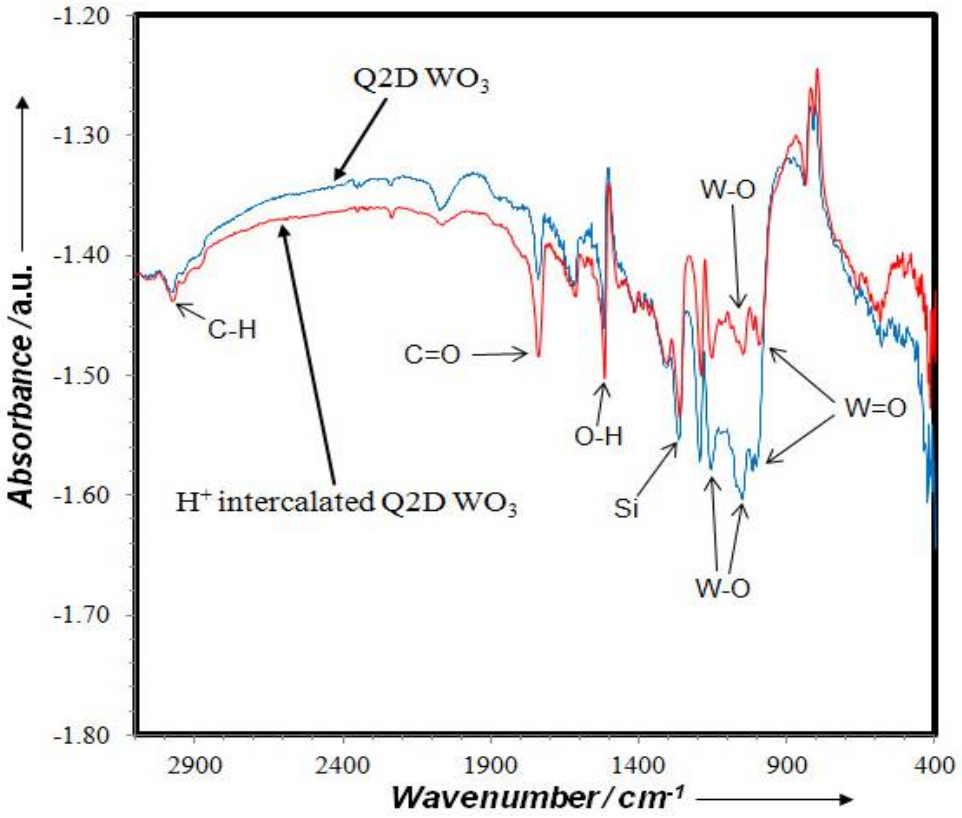

Figure S6. *In-situ* FTIR spectra for exfoliated Q2D WO_3 and H^+ intercalated Q2D WO_{3-x} nano-flakes.

Supporting References

1. T. Ando, A. B. Fowler and F. Stern, *Rev. Mod. Phys*., 1982, **54**, 437-672.
2. S. Balendhran, J. Deng, J. Z. Ou, S. Walia, J. Scott, J. Tang, K.L. Wang, M.R. Field, S. Russo, S. Zhuiykov, M.S. Strano, N. Medhekar, S. Sriram, M. Bhaskaran and K. Kalantar-zadeh, *Adv. Mater*., 2013, **25**, 109-114.
3. M. Osada and T. Sasaki, *Adv. Mater*., 2012, **24**, 210-223.
4. D. K. Schroder, Semiconductor material and device characterisation, Wiley, 3d ed. 2006, 800.
5. A. Davydov, *Molecular Spectroscopy of Oxide Catalyst Surfaces* Wiley, 2003, 670.
6. S. M. Kanan, Z. Lu, J. K. Fox, G. Bernhardt and C. P. Tripp, *Langmuir*, 2002, **18**, 1707-1712.
7. Z. Lu, S. M. Kanan and C.P. Tripp, *J. Mater. Chem*., 2002, **12**, 983-989.
8. P. Hollins, *Suf. Sci. Rep*., 1992, **16**, 51-94.
9. U. Opara-Krasovec, R. Jese, B. Orel, J. Grdadolnik and G. Drazic, *Monatshefte Fur Chemie*, 2002, **133**, 1115-1133.